MODELLING SHORT-TERM SPECTRAL IRRADIANCE VARIATIONS

M. FLIGGE[1], S.K. SOLANKI[1,2] and Y.C. UNRUH[3]
[1]*Institute of Astronomy, ETH Zentrum, CH-8092 Zurich, Switzerland*
[2]*Max-Planck-Institut für Aeronomie, D-37191 Katlenburg-Lindau, Germany*
[3]*Institut für Astronomie, Universität Wien, Türkenschanzstr. 17, A-1180 Wien, Austria*

Received: 19 October 1999; Accepted in final form: 23 December 1999

Abstract. On time-scales of the solar rotation most of the solar irradiance variations are caused by the changing distribution of solar surface magnetic features. We model these short-term irradiance variations using calculations of sunspot and facular contrasts as a function of wavelength and limb angle on the Sun. The position of active regions on the solar disc is derived from the MDI magnetograms. The reconstructed irradiance variations are compared with total and spectral irradiance measurements obtained by the VIRGO experiment on SOHO.

1. Introduction

Within the flux-tube picture of the magnetic field (Solanki, 1993), the average brightness of solar magnetic features is mainly a function of two parameters: the size of the magnetic feature and its position on the Sun (Knölker and Schüssler, 1988; Solanki, 1993 and references therein). For observations that cannot resolve individual small flux tubes (and the full-disk maps used in this study are of this type), the flux-tube size can be replaced by the magnetic filling factor (Solanki and Brigljević, 1992) which is simply the fraction of the solar surface within a given pixel of the map covered by magnetic flux tubes. Solar irradiance variations are then basically explained by the changing surface area coverage and distribution of magnetic features like sunspots and faculae, at least on the time-scales considered here.

The irradiance reconstruction presented here makes use of sunspot and facular contrasts calculated as a function of wavelength and limb angle on the Sun (Unruh et al., 1999; henceforth called USF99) using Kurucz's ATLAS9 spectral synthesis code (Kurucz, 1992a, 1992b, 1992c). The position and size of magnetic features on the solar disk are extracted from full-disk magnetograms and continuum intensity images obtained by the Michelson Doppler Interferometer (MDI) onboard the Solar and Heliospheric Observatory (SOHO) spacecraft.

In the discussions to follow we first briefly introduce our 3-component model of solar surface magnetism and sketch how we calculate irradiance variations in Sect. 2. We present the calculated total and spectral irradiance variations in Sect. 3 where we also compare them to measurements obtained by the Variability of Irradi-

Space Science Reviews **94:** 139–144, 2000.

ance and Gravity Oscillations (VIRGO) experiment onboard the SOHO spacecraft. Finally, we summarize our results in Sect. 4.

2. Model

The general modeling procedure is as follows: First, magnetic maps are created by decomposing magnetograms into sunspot, facular and quiet Sun regions. The value of the magnetic flux for each pixel is converted into a corresponding filling factor taking the limited spatial resolution of the magnetogram into account. Then, each pixel is replaced by a corresponding intensity value that depends on the filling factor and position on the solar disk. Finally, by summing the intensities over the full solar disk, the value for the irradiance is obtained.

We divide the solar surface into 3-components, namely quiet Sun I^q, sunspots I^s and faculae I^f, whose intensities I depend on the cosine of the limb angle μ and wavelength λ, but do not otherwise change with time t. The 3-components are employed for each solar surface element, i.e. each pixel of a magnetogram. The intensities are calculated for eleven different limb angles from $\mu = 1.0$ (disk center) to the very limb ($\mu = 0.05$) following USF99.

The intensity $I^{\mathrm{tot}}_{i,j}(\lambda; t)$ of a given element (i,j) on the solar disk at time t and wavelength λ is then given by:

$$\begin{aligned} I^{tot}_{i,j}(\lambda; t) \;=\; [1 - \alpha^s_{i,j}(\Phi; t) \;-\; \alpha^f_{i,j}(\Phi; t)] \;&\cdot I^q(\mu(i, j), \lambda) \\ +\; \alpha^s_{i,j}(\Phi; t) \;&\cdot I^s(\mu(i, j), \lambda) \\ +\; \alpha^f_{i,j}(\Phi; t) \;&\cdot I^f(\mu(i, j), \lambda), \end{aligned} \tag{1}$$

where $\alpha^s_{i,j}(\Phi; t)$ and $\alpha^f_{i,j}(\Phi; t)$ are the filling factors per surface element for sunspots and faculae, respectively, which are extracted from MDI magnetograms and continuum intensity images. After correcting for fore-shortening (magnetograms) and center-to-limb variations (continuum intensity images), respectively, a simple threshold criterion is used to select facular and sunspot pixels. Then, the magnetic flux density Φ (measured by the magnetogram) of each selected pixel is converted into a corresponding filling factor α.

Sunspots are well resolved by the full-disk MDI magnetograms and since stray light plays a minor role in the seeing-free environment of MDI we set $\alpha^s_{i,j}(\Phi) = 1$ for each pixel (i, j) within a sunspot.

For faculae, the situation is more complex. Faculae originate from more loosely packed magnetic elements (flux-tubes). At least for small facular regions (with low magnetic flux density) the filling factor is smaller than 1 and an appropriate scheme which converts magnetic flux densities into filling factors must be applied. We stress that the meaning of the filling factor used here differs from the usually employed magnetic filling factor. The latter has a considerably smaller value.

The conversion scheme we have employed is illustrated in Fig. 1. We increase the facular filling factor α^f linearly from zero at Φ_{th} to 1.0 at Φ_{sat}. The threshold

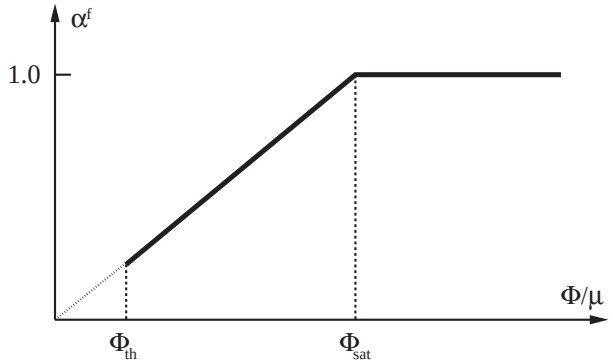

Figure 1. Conversion of magnetic flux Φ measured within a pixel of a magnetogram into a corresponding facular filling factor α^f. The facular filling factor α^f increases linearly from zero at $\Phi_{\rm th}$ to 1.0 at $\Phi_{\rm sat}$.

$\Phi_{\rm th}$ separates the signal from the noise within the magnetogram. For magnetic flux densities larger then $\Phi_{\rm sat}$, however, α^f remains unity. The reason for introducing this saturation lies in the observation that the average temperature enhancement within flux tubes relative to the quiet Sun decreases with increasing filling factor (Hirayama, 1978; Solanki and Stenflo, 1984; Solanki and Brigljević, 1992). Since we describe all faculae by the same thermal structure the simplest, although not particularly accurate way of accounting for the above observations in our model is by introducing a saturation in $\alpha^f(\Phi)$. For the results discussed in the following we employ $\Phi_{\rm sat} = 100$ G which means that already relatively weak faculae originate from densely packed magnetic elements.

As a result we get the filling factor maps $\alpha_s(\Phi; t)$ for sunspots and $\alpha_f(\Phi; t)$ for faculae. The total intensity of each pixel, $I^{tot}_{i,j}(\lambda; t)$, can then be calculated according to Eq. (1). Finally, relative solar irradiance variations are obtained from the relation:

$$\frac{\Delta S_\lambda}{S_\lambda} = \frac{\sum_{i,j} I^{tot}_{i,j}(\lambda) - \sum_{i,j} I^q(\mu(i,j),\lambda)}{\sum_{i,j} I^q(\mu(i,j),\lambda)}. \tag{2}$$

To model VIRGO measurements we constrain the wavelengths to the desired spectral band by multiplying the intensities $I^{\rm tot}_{i,j}(\lambda)$ and $I^q(\mu(i,j),\lambda)$ with the appropriate transmission function for each of the three spectral filters prior to integration over wavelength (Fligge et al., 1998).

3. Results

In the following, we present two reconstructions of solar total and spectral irradiance variations over the periods 15 August 1996–15 September 1996 and 6 November 1996–6 January 1997 and compare them to VIRGO measurements

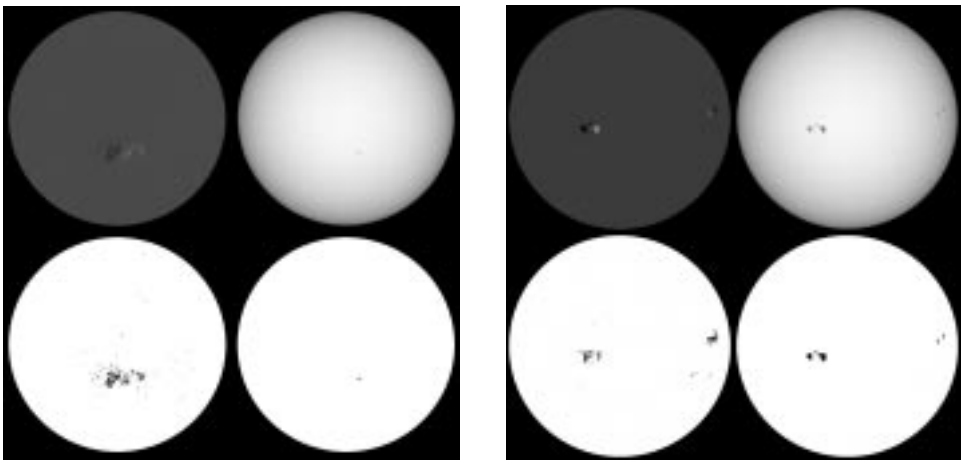

Figure 2. Extraction of sunspot and facular regions from a magnetogram. Left panel: The magnetogram (upper left) and the corresponding continuum intensity image (upper right) were taken on 30 August, 1996 by MDI. Below are the extracted maps for faculae (lower left) and sunspots (lower right). The decaying active region visible on the solar disk is dominated by faculae, although a small spot is also present. Right panel: Same, but for 25 November, 1996.

of total and spectral irradiance at 402 nm, 500 nm and 862 nm, respectively. At this time the Sun was still very close to activity minimum, making it particularly suitable for a detailed study of the influence of single active regions on irradiance variations unhampered by the presence of other active regions.

Fig. 2 shows the extraction of sunspot and facular regions for two days, i.e. 30 August 1996 (left panel) and 25 November 1996 (right panel), respectively. The upper two images of each panel show the magnetogram (left) and continuum intensity image (right) recorded by MDI. Below are the extracted maps for faculae (lower left) and sunspots (lower right), i.e. α_f and α_s. The first period is mainly faculae-dominated while during the second period an active region harboring two large sunspots showed up on the disc.

The reconstructed (solid lines) and measured (dashed lines) irradiance variations are presented in Fig. 3.

The model is able to reconstruct irradiance variations on time-scales of the solar rotation and reproduces the double-peaked structure originating from the center-to-limb variation (CLV) of the facular brightening rather well. The model yields linear correlation coefficients between the observed and modeled time-series of 0.98, 0.92, 0.93 and 0.90 for the total, blue, green and red channels, respectively. For comparison, the dotted curve shows an earlier reconstruction which neglects the CLV of the facular contrast (Fligge et al., 1998). Quite clearly, the new reconstruction, based on magnetograms and the CLV of intensity spectra is far superior.

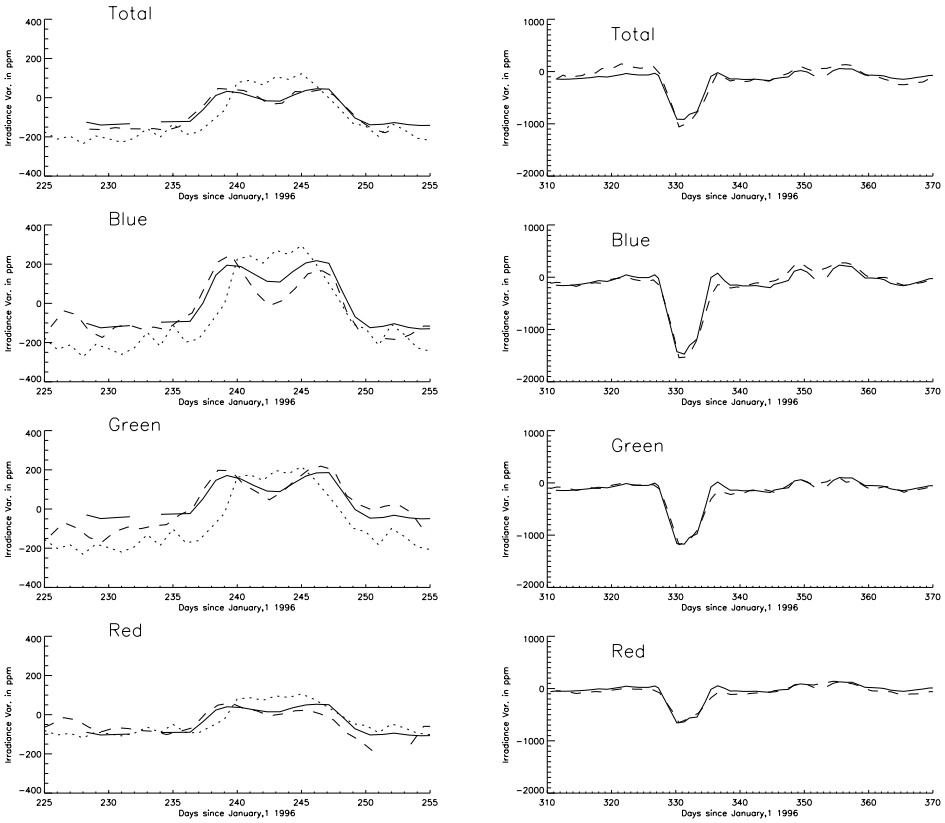

Figure 3. Comparison between measured (solid) and modeled (dashed) solar total and spectral irradiance variations for the time between 15 August and 15 September 1996 (left panel) and 6 November 1996 and 6 January 1997 (right panel), respectively. Plotted are (from top to bottom) a) the total irradiance, and the spectral irradiance variations measured in b) the blue, c) green and d) red color channels of VIRGO. Our model reproduces the double-peaked structure originating from the CLV of the facular contrast (left panel). However, some deviations from the measurements remain unexplained. For comparison, the dotted curve in the left panel shows a reconstruction which neglected the CLV of the facular contrast. The dimming of solar irradiance due to the passage of sunspots (right panel) is also well reproduced.

4. Conclusions

We present a model of solar total and spectral irradiance variations based on a 3-component model which includes the center-to-limb variation of the brightness of magnetic features. It makes direct use of magnetic maps (together with calculated intensity spectra) to reconstruct irradiance rather than proxies, such as Ca II K, Mg II k or He I 10830 Å indices which are formed in chromospheric layers. This requires detailed calculations of intensity spectra for each of the three atmospheric components as a function of wavelength and limb angle described in USF99. This

approach is able to significantly improve reconstructions of irradiance variations on time-scales of the solar rotation relative to models based on disk-integrated proxies.

We wish to point out that spectra from the same atmospheric models of quiet Sun, sunspots and faculae as we use, also reproduce a number of other observations, such as the variation of the UV spectral irradiance between solar minimum and maximum, the ratio of facular to spot area, the fraction of irradiance variations due to line blanketing, etc. (see USF and Unruh et al., 2000, for more details).

The success of our model further strengthens the hypothesis that the magnetic field is the dominant driver of solar irradiation variations, at least on the short time scales considered in this paper. In order to further fine-tune the input parameters of our model, increase the statistical significance of the reconstructions and test our basic assumptions, longer time intervals have to be considered which, preferentially, should cover different levels of solar activity.

References

Fligge, M., S. K. Solanki, Y. C. Unruh, C. Fröhlich, and C. Wehrli: 1998, 'A model of solar total and spectral irradiance variations'. *Astron. Astrophys.* **335**, 709–718.

Hirayama, T.: 1978, 'A Model of Solar Faculae and Their Lifetime'. *Publ. Astron. Soc. Jpn.* **30**, 337–352.

Knölker, M. and M. Schüssler: 1988, 'Model calculations of magnetic flux tubes. IV - Convective energy transport and the nature of intermediate size flux concentrations'. *Astron. Astrophys.* **202**, 275–283.

Kurucz, R. L.: 1992a, 'Atomic and molecular data for opacity calculations'. *Revista Mexicana de Astronomia y Astrofisica* **23**, 45–48.

Kurucz, R. L.: 1992b, 'Finding the 'Missing' solar ultraviolet opacity.'. *Revista Mexicana de Astronomia y Astrofisica* **23**, 181–186.

Kurucz, R. L.: 1992c, 'Remaining line opacity problems for the solar spectrum'. *Revista Mexicana de Astronomia y Astrofisica* **23**, 187–194.

Solanki, S. K.: 1993, 'Small scale solar magnetic fields - an overview'. *Space Science Reviews* **63**, 1–188.

Solanki, S. K. and V. Brigljević: 1992, 'Continuum brightness of solar magnetic elements'. *Astron. Astrophys.* **262**, L29–L32.

Solanki, S. K. and J. O. Stenflo: 1984, 'Properties of solar magnetic fluxtubes as revealed by Fe I lines'. *Astron. Astrophys.* **140**, 185–198.

Unruh, Y. C., S. K. Solanki, and M. Fligge: 1999, 'The spectral dependence of facular contrast and solar irradiance variations'. *Astron. Astrophys.* **345**, 635–642.

Unruh, Y. C., S. K. Solanki, and M. Fligge: 2000, 'Modelling solar spectral irradiance variations', *Space Sci. Rev.*, this volume.

Address for Offprints: M. Fligge, Institute of Astronomy, ETH Zentrum, CH-8092 Zurich, Switzerland. fligge@astro.phys.ethz.ch